

In situ production of pre-vascularized synthetic bone grafts for regenerating critical-sized defects in rabbits

Luciano Vidal, Meadhbh Á Brennan, Stéphanie Krissian, Julien de Lima, Alain Hoornaert, Philippe Rosset, Borhane H Fellah, Pierre Layrolle

▶ **To cite this version:**

Luciano Vidal, Meadhbh Á Brennan, Stéphanie Krissian, Julien de Lima, Alain Hoornaert, et al.. In situ production of pre-vascularized synthetic bone grafts for regenerating critical-sized defects in rabbits. Acta Biomaterialia, 2020, 114, pp.384 - 394. ⟨10.1016/j.actbio.2020.07.030⟩. ⟨hal-03492265⟩

HAL Id: hal-03492265

https://hal.science/hal-03492265v1

Submitted on 5 Sep 2022

HAL is a multi-disciplinary open access archive for the deposit and dissemination of scientific research documents, whether they are published or not. The documents may come from teaching and research institutions in France or abroad, or from public or private research centers.

L'archive ouverte pluridisciplinaire **HAL**, est destinée au dépôt et à la diffusion de documents scientifiques de niveau recherche, publiés ou non, émanant des établissements d'enseignement et de recherche français ou étrangers, des laboratoires publics ou privés.



Distributed under a Creative Commons CC BY-NC 4.0 - Attribution - Non-commercial use - International License

Version of Record: https://www.sciencedirect.com/science/article/pii/S1742706120304165
Manuscript_467243fd1c2a02ab5072b62766ee12d0

In situ production of pre-vascularized synthetic bone grafts for regenerating critical-sized defects in rabbits

Luciano Vidal, MD, PhD [1, §;] Meadhbh Á Brennan, PhD [1,2, §]; Stéphanie Krissian, MD [1,3]; Julien De Lima [1]; Alain Hoornaert, DDS, PhD [1,4]; Philippe Rosset, MD, PhD [1,3]; Borhane H Fellah, DVM, PhD [5]; Pierre Layrolle, PhD [1*]

1) Inserm, UMR 1238, PHY-OS, Bone sarcomas and remodeling of calcified tissues, Faculty of Medicine, University of Nantes, 1 rue Gaston Veil, 44035 Nantes, France.
2) John A. Paulson School of Engineering and Applied Sciences, Harvard University, Cambridge, MA, USA
3) CHRU Tours, Department of trauma and orthopedic surgery, Hospital Bretenneau, 2 Boulevard Tonnelé, 37000 Tours, France
4) CHU Nantes, Department of Implantology, Faculty of Dentistry, University of Nantes, 1 Place Alexis Ricordeau, 44042 Nantes, France
5) ONIRIS, CRIP, Veterinary School, 101 route de Gachet, 44307 Nantes, France

§ These authors contributed equally to this work

*** Corresponding author**

Prof. Pierre Layrolle, PhD, Director of Research, Inserm, UMR 1238, PHY-OS, Bone sarcomas and remodeling of calcified tissues, Faculty of Medicine, University of Nantes, 1 rue Gaston Veil, 44035 Nantes, France, email: pierre.layrolle@univ-nantes.fr

Original manuscript prepared for submission to the Journal **Acta Biomaterialia**

Date of the initial submission: March 10, 2020

© 2020 published by Elsevier. This manuscript is made available under the CC BY NC user license
https://creativecommons.org/licenses/by-nc/4.0/

Abstract

Reconstructing large bone defects caused by severe trauma or resection of tumors remains a challenge for surgeons. A fibula free flap and its vascularized bed can be transplanted to the reconstruction site to achieve healing. However, this technique adds morbidity, requires microsurgery and sculpting of the bone tissue to adapt the graft to both the vasculature and the anatomy of the defect respectively. The aim of the current study is to evaluate an alternative approach consisting of the *in situ* production of a pre-vascularized synthetic bone graft and its subsequent transplantation to a critical-sized bone defect. 3D printed chambers containing biphasic calcium phosphate (BCP) granules, perfused by a local vascular pedicle, with or without the addition of stromal vascular fraction (SVF), were subcutaneously implanted into New Zealand White female rabbits. SVF was prepared extemporaneously from autologous adipose tissue, the vascular pedicle was isolated from the inguinal site, while BCP granules alone served as a control group. After 8 weeks, the constructs containing a vascular pedicle exhibited abundant neovascularization with blood vessels sprouting from the pedicle, leading to significantly increased vascularization compared to BCP controls. Pre-vascularized synthetic bone grafts were then transplanted into 15 mm critical-sized segmental ulnar defects for a further 8 weeks. Micro-CT and decalcified histology revealed that pre-vascularization of synthetic bone grafts led to enhanced bone regeneration. This pre-clinical study demonstrates the feasibility and efficacy of the *in situ* production of pre-vascularized synthetic bone grafts for regenerating large bone defects, thereby addressing an important clinical need.

Keywords:

Bone regeneration; vascularization; vascular pedicle, biphasic calcium phosphate; 3D printing; implantable chamber; bone graft transplantation.

Introduction

Although minor fractures and small bone defects can heal spontaneously, large and complex bone defects have limited capacity for regeneration. Reconstructing large bone defects that are the result of severe trauma or tumor ablation remains a critical challenge for orthopedic and plastic surgeons [1]. Autologous bone grafting, whereby bone tissue is harvested from one site and transplanted into the defect site, is currently the gold standard procedure for regenerating large bone defects. Adequate vascularization is recognized as being a pivotal factor in ensuring the viability of a bone graft and the subsequent healing of the defect, indeed there is a statistically significant positive correlation between vascularization and bone formation [2]. Consequently, vascularized bone grafts are required for the regeneration of large bone defects. Free flaps, comprising harvested bone from sources such as the radius or fibula, together with a vascular supply and soft tissue, can be transplanted into the reconstruction site, where they are connected to the local vasculature [3]. Vascularized bone transfers have demonstrated faster healing, higher resistance to resorption, and superior mechanical integrity than non-vascularized bone grafts [4]. However, this transplantation technique is associated with serious limitations. Firstly, the geometry of the graft rarely conforms to the shape and size of the bone defect, thereby requiring bone sculpting to attain an anatomically correct shape. Furthermore, connecting the vasculature of the graft to the vasculature of the defect site requires extensive microsurgery. Finally, the quantity of bone and soft tissue available to harvest from the donor site is limited, and most importantly, harvesting bone and surrounding tissue for grafting causes extreme pain and morbidity for the patient [5].

A major goal for orthopedic reconstructive surgery is therefore to avoid the need for the creation of a second surgical bone harvest site by using synthetic biomaterials as an alternative to grafted autologous bone. Synthetic biomaterials alone do not have the adequate

osteoinductive or angiogenic properties for healing large bone defects. However, osteoprogenitor/stem cells, in particular mesenchymal stromal/ stem cells derived from bone marrow (BMSCs), combined with biomaterials, have been successful in regenerating bone tissue [6–9]. Nevertheless, it is well established that the lack of vascularization within a synthetic bone construct is the most critical obstacle to healing large bone defects [10]. Proximity to a vascular network is vital for cell viability, and sufficient delivery of nutrients and oxygen. Consequently, necrosis is often observed in the center of large synthetic implants as there is not enough extrinsic vascularization to produce vessel in-growth from the surrounding host tissue fast enough [11].

The aim of pre-vascularized synthetic constructs is to overcome the challenges of autologous bone grafting of free flaps and of synthetic biomaterial constructs. In the tissue engineering context, various efforts have been made to produce a network of blood vessels in vitro that has the capacity to anastomose after transplantation *in vivo* in order to deliver sufficient nutrients to the cells within the scaffold, thus enhancing their survival and functionality after implantation. The most sophisticated strategies target the delivery of MSCs together with endothelial cells, and *in vitro* these constructs have more advanced osteoblastic and endothelial differentiation compared to groups containing a single cell type [12]. However, when implanted into bone defects, these multicellular constructs did not enhance bone regeneration compared with the delivery of MSCs alone [13,14]. Recent work using 3D bio-printing has led to the creation of a perfusable vascular network using bio-inks and endothelial cells [15–17]. This approach seems promising, although it is still a long way from clinical applications.

In situ-generated synthetic vascularized constructs have many advantages over the complex and labor-intensive culture required for *in vitro* generation of tissue-engineered vascularized constructs. Several teams have suggested prefabricating synthetic bone substitutes by means

of ectopic implantation, making pre-vascularization possible according to an '*in vivo* bioreactor' principle before transplanting it into the defect to be regenerated. To date, various strategies have been investigated to achieve pre-vascularization. Muscle tissue, which has a rich capillary network, has been wrapped around scaffolds in the form of an intramuscular pouch to encourage vessels to sprout from the muscle into the construct. Since this technique was first reported [18] its use has generated constructs with enhanced vascularization [19] however, its success was limited in pre-clinical and clinical studies by core necrosis [19,20]. This technique, along with adipose tissue derived stromal cells (ATSCs) and BMP-2, has nevertheless demonstrated success in large maxillofacial defect reconstruction [21]. Arteriovenous (AV) loops have been used successfully to generate large vascularized synthetic constructs using fibrin matrix [22], coral scaffolds [23] and ceramics [24] in ectopic sites in animals. Recently, it was demonstrated that a ceramic construct, pre-vascularized using an AV loop in an ectopic site, showed superior bone healing following transplantation into a bone defect, compared to the construct without pre-vascularization [25]. However, in spite of these favorable outcomes, the applicability of the AV loop is restricted by the intricate microsurgical skills required for the construction of the arteriovenous shunt.

An alternative strategy to an AV loop is to provide vascularization by using a vascular pedicle. In this model, an artery and a vein are inserted centrally within an implantable chamber containing the biomaterial scaffold. The isolation of a vascular pedicle is relatively simple and does not require anastomosis of the blood vessels, thereby circumventing the complicated microsurgery required for an AV loop. An arteriovenous vascular bundle placed inside a construct with cadaver bovine bone [26] or autologous ovine bone and bone marrow [27], achieved a fully-vascularized construct in ectopic sites in rats and sheep respectively. Further to this, chambers containing synthetic ceramic biomaterial with a vascular bundle, and growth factors [28] or BMSCs implanted ectopically demonstrated abundant

microvasculature and tissue engineered bone [29,30]. Together, these studies demonstrate the utility of a pre-vascularized construct generated by using a vascular bundle. However, evaluation of the performances of this type of construct following transplantation into a large bone defect has not yet been conducted.

The objective of this study was to produce a highly vascularized graft *in situ* and to transplant it into a critical-sized defect in rabbits for bone reconstruction. In the current study, we used biphasic calcium phosphate (BCP) granules as the synthetic biomaterial, as this material has been shown in pre-clinical [6] and clinical studies [31,32] to be a suitable scaffold for bone healing. While ligated vascular pedicles can also achieve pre-vascularization constructs [30], we choose not to ligate the vascular pedicle due to increased risk of thrombosis. In line with our aim to prefabricate a graft with abundant microvasculature, we chose to also deliver autologous stromal vascular fraction (SVF) isolated from adipose tissue, because similarly to human-derived SVF [33,34], SVF from rabbits contains cells such as MSCs and endothelial cells [35,36]. The delivery of these cells has previously shown to stimulate angiogenesis in rabbits [37,38] and other animal models [39–41]. The principal advantage of delivering SVF instead of expanded MSCs from adipose tissue is that the preparation the SVF could be performed extemporaneously in a single surgery, whereas the delivery of ATSCs requires *in vitro* expansion and hence a second surgery. Chambers containing the BCP granules and a local vascular pedicle inserted centrally, with or without SVF supplementation, were implanted subcutaneously into New Zealand White (NZW) female rabbits. After 8 weeks, the constructs were characterized by micro-computer tomography (μCT), immunohistochemistry and histology for vascularization and bone tissue formation. In a second operative step, the bone construct was transplanted into a mid-diaphyseal segmental ulna defect, a critical-sized defect which has been previously described [42–44]. After a further 8 weeks, the animals

were euthanized, and samples were analyzed by μCT and decalcified histology for bone regeneration.

Materials and Methods

Biomaterials

Implantable chambers, to hold the synthetic biomaterials, SVF, and vascular pedicle, were designed using computer-aided design software (CAD, Space Claim Corporation, Concord, Massachusetts, USA). Chambers consisting of hollow cylinders measuring 15 mm in length and 10 mm in diameter, with a wall thickness of 1 mm, were designed to contain the BCP granules. A transversal window, measuring 3.5 mm in width and 15 mm in length, with two openings of 4.5 mm in diameter, was made to allow the vascular pedicle to pass through the implantable chamber. The drawing was exported in stereo lithography format (STL) and converted into a readable G-code file (Cura software). The implantable chambers were printed in 3D using polylactic acid (PLA) white filament, 3 mm in diameter (Ultimaker 2, Ultimaker B.V, Geldermalsen, The Netherlands). After 3D printing, the implantable chambers were deburred, cleaned with 70% ethanol, and air-dried. The sterilization of the chambers was ensured by immersion for 1 hour in a solution of glutaraldehyde followed by washing in a saline solution.

The synthetic bone substitute used in this study was macro- and micro-porous BCP (Biomatlante, Vigneux de Bretagne, France) in the form of irregular granules measuring 0.5-1 mm in size. These BCP granules were prepared by mixing calcium-deficient apatite with pore makers, compacting the material, sintering at 1050 °C, crushing and sieving. The BCP granules were composed of 20 % hydroxyapatite (HA) and 80 % beta tricalcium phosphate (β-TCP) in weight as analyzed by X-ray diffraction. The BCP granules had an overall porosity of 70 %, consisting of macropores (>100 µm) and micropores (10< µm), as measured by mercury intrusion porosimetry [45]. The BCP granules were sterilized by gamma irradiation at a dose > 25 kGy.

In order to avoid bone regeneration of the ulna defect from the periosteum of the radius, a bi-

layer membrane of polylactic glycolic acid (PLGA, Tisseos®, Biomedical Tissues, Nantes, France) was placed between the radius and ulna. This synthetic resorbable bi-layered membrane was manufactured from medical grade PLGA copolymer (Purasorb PLG 8531, Corbion Purac BV, Gorinchem, The Netherlands) using a proprietary process in a clean room [46]. The PLGA membrane, 10 × 20 mm in size, was packaged in double-sealed pouches and sterilized with gamma irradiation at 25 kGy (Ionisos SA, Dagneux, France).

Study design and ethical approval

The study involved a total of 25 NZW rabbits in two surgical phases. The experiments were conducted in accordance with European Directive 2010/60/EU. Ethical approval for this study was obtained from the local ethics committee (CEEA, Pays de Loire, France) under the authorization project numbers CEEA.2012.119 and Apafis # 1917. The experiments were carried out at the Preclinical Investigation Research Center (CRIP) of the National Veterinary School of Nantes (ONIRIS, Nantes, France) under the supervision of a doctor in veterinary medicine. NZW adult female rabbits with a body weight of 4.5 kg were purchased from a professional breeder (Hypharm, Roussay, France). The animals were housed in individual cages with unlimited water and food. The room was ventilated and air-conditioned to a temperature of 20 ± 1 °C. An artificial day / night cycle of 12 h was applied. The rabbits were acclimated for at least 10 days prior to surgery. In the first surgery, two chambers containing the BCP granules and a central vascular pedicle, with or without supplementation with autologous SVF, were implanted into inguinal sites. Adipose tissue was collected and processed for preparation of the SVF during the first surgery. Chambers containing BCP alone served as controls. Each rabbit received two implants, with groups defined according to the content of the implanted chambers: synthetic bone filler alone (BCP), BCP with a vascular pedicle (BCP + Pedicle), or BCP supplemented with autologous SVF and a vascular pedicle

(BCP + SVF + Pedicle). One group of rabbits was sacrificed after 8 weeks in order to evaluate the vascularization inside the chambers by μCT. The second surgery was performed on 19 rabbits. 12 rabbits that had received two subcutis chambers containing BCP + Pedicle (n=6) and BCP + SVF + Pedicle (n=6) for 8 weeks were re-operated on for transplantation of the content of the chambers into ulnar defects. The rabbits were placed under general anesthesia and the chambers were explanted from the inguinal subcutis sites. The outer 3D-printed PLA chamber was removed and the content was transplanted into the ulna defect. The second chamber was collected and fixed in buffered formaldehyde for histological evaluation. A further seven rabbits of the same age and body weight were used for creation of ulnar defects that were left empty (n=3) or filled with BCP granules (n=4). Eight weeks after the second surgery, the animals were euthanatized. The ulnas were dissected and immediately fixed in buffered formaldehyde for μCT and histology.

Subcutis implantation of chambers in rabbits

The rabbits were placed under general anesthesia by means of an intramuscular injection of a mixture of xylazine (Rompun® 2%, 0.2 mg / kg, Bayer Pharma, Puteaux, France) and ketamine (Imalgène 1000®, 20 mg / kg, Mérial, Lyon, France). The inguinal sites were shaved and disinfected with povidone and sterile gauzes, and sterile fields were set up to delimit the surgical area. The general anesthesia was maintained by the intravenous injection of the same mixture through a catheter placed in the marginal vein of the ear. The rabbit was monitored for body temperature and heart pulse during the surgery. The primary surgical steps for inguinal subcutis implantation are shown in Figure 1. A medial cutaneous incision measuring 3- 4 cm was made in the inguinal region. Two identical chambers were implanted into the subcutaneous inguinal sites of each rabbit. In control samples, BCP was added directly to the chambers (BCP). In the case of pre-vascularized implants, two pedicles were

isolated from the left and right femoral artery branches respectively. The dissection of the femoral artery was performed in deep planes in the inguinal site. Once the branch of the femoral artery was identified, delicate dissection of the pedicle was conducted with careful hemostasis by using an electrical bistoury. Some BCP particles were loaded into the chamber, then the vascular pedicle was placed in the transverse position and the chamber was then completely filled with BCP granules, taking care not to compress the blood vessel. Hemostasis and the patency of the vessels upstream and downstream of the chamber were verified. After smooth dissection of the subcutaneous connective tissue, 6g of adipose tissue adjacent to the mammary tissue was harvested and processed for isolation of the SVF. While harvesting the adipose tissue, hemostasis was ensured by using an electric scalpel. Preparation of the SVF required less than 1 hour while the rabbit was maintained under general anesthesia, with the open wound moistened with saline gauzes. Chambers with a vascular pedicle were filled with BCP granules alone (BCP + Pedicle) or BCP granules mixed with SVF (BCP + SVF + Pedicle). All chambers were fixed to the abdominal muscle with non-absorbable sutures (Prolene®, 2/0, Ethicon). The surgical site was closed in layers using subcutaneous and cutaneous sutures with resorbable braided sutures (Polysorb Dec.2®, 2/0 and 3/0, Tyco Healthcare). Post-operative analgesia was provided by a transdermal patch of Fentanyl (Durogesic®, 15 µg/kg/h) placed on the ear, ensuring continuous release of the active substance for 3 to 5 days. Post-operative s.c. injection of non-steroidal anti-inflammatory drugs (Meloxicam, Metacam®, Boehringer-Ingelheim, Reims, at a dose of 0.1 to 0.2 mg/kg/day) was administered for 5 days. An antibiotic treatment of marbofloxacin (3 mg/kg, s.c. injection, Marbocyl, Vetoquinol, Paris, France) was started the day of surgery and repeated for 5 days. After surgery, the animals were monitored for signs of suffering, and the surgical wounds were inspected daily to check for skin healing and the absence of infections.

Extemporaneous preparation and characterization of the stromal vascular fraction of adipose tissue from rabbits

Autologous adipose tissue (AT), 6 g per rabbit, was harvested in the inguinal-abdominal region of rabbits during the first surgery. The AT was placed in a sterile 50 ml tube (Falcon, BD). The SVF was prepared in aseptic conditions under a laminar flow cabinet. The AT was washed three times with phosphate buffered saline (PBS, Gibco) to eliminate red blood cells. Mechanical digestion was performed to roughly dissociate the AT with scissors and vortexing for 1 to 2 minutes. Enzymatic digestion was performed with 0.075% collagenase A (Roche) at 37 °C for 45 min with 3 vortex agitations for 1 to 2 min. After digestion, the yellow viscous solution was filtered through 70 µm (Becton-Dickinson), to remove tissue debris, and centrifuged at 1600 rpm for 5 min. After removal of the oily supernatant, the cell pellet corresponding to the SVF was suspended in 1.5 ml of PBS to allow it to associate with the BCP granules. The SVF was implanted subcutaneously into the same rabbit as the harvested AT sample to avoid an immune response against allogeneic cells. Cell counting of the SVF preparation was performed using an automated cell counter (Nucleocounter® NC-100, Denmark).

In order to demonstrate their multi potency, 1.5 x 10^5 nucleated cells from the SVF of rabbits were cultured in a 75 cm^2 flask in Dulbecco's modified Eagle-based culture medium (Gibco® DMEM, Life Technologies, Inc. Saint Aubin, France) supplemented with 10% fetal calf serum (FCS, GE Healthcare, Vélizy-Villacoublay, France) and 1% penicillin / streptomycin (Gibco) at 37 °C in a humidified atmosphere (5% CO_2 / 95 % of air). The culture medium was refreshed every 2-3 days. After 7 days of culture, the adherent cells (ATSCs) were approximately 80 % confluent and were detached from the plastic by trypsin/EDTA (Lonza, Belgium) and centrifuged at 1600 rpm for 5 min (Passage 0). After cell counting, the cells were amplified in a 500 cm^2 triple flask at a cell density of 5 × 10^3 cells/cm^2 for 7 days

(passage 1). After detachment and counting, the cells were cultured in 24-well plates at an initial cell density of 2×10^4 and 5×10^3 cells/cm^2 under adipogenic and osteogenic conditions respectively, with 500 µL of differentiation media (StemPro® Differentiation kits, Life Technologies, Saint Aubin, France). For chondrocyte differentiation, 1 x 10^6 ATSCs were pelleted at 1600 rpm for 5 min and pellets were cultured under standard chondrogenic conditions (StemPro kits ®Differentiation). The culture medium was refreshed every 2-3 days. After 21 days of culture, cells were fixed in 4% paraformaldehyde. Staining with oil red O (M312512, Fisher), Alizarin red (Sigma Aldrich) and Alcian blue (Sigma Aldrich) was performed to highlight, respectively, the presence of adipocytes, the mineralized matrix produced by osteoblasts, and glycosaminoglycans produced by chondrocytes.

Transplantation of the pre-vascularized bone grafts into the ulnar defects

Eight weeks after implanting the chambers into the inguinal site, a second surgery was performed. The rabbits were placed under general anesthesia and prepared for surgery as previously described. The chambers containing the pre-fabricated synthetic bone grafts were exposed by smooth dissection. The chambers were removed after verifying that the permeability of the pedicles was being maintained, and placement of the vascular ligatures. The vascular permeability was assessed by clamping and sectioning the distal end of the pedicle, and after unclamping by observation of the bleeding of the pedicle. As shown in Figure 2, the vascularized synthetic grafts were gently removed from the PLA breakable chambers and stored in a sterile gauze moistened with physiological saline for transplantation into the ulna defect. The second construct resected from each rabbit was put in 10% formalin fixative for further analysis by histology. In the second surgery, the osseous site was prepared to create a critical size segmental defect at the mid-diaphysis level of the left ulna. One critical-sized defect site per rabbit was created as previously described [42–44]. The surgical

approach was performed caudo-laterally with respect to the ulna in its middle third, so as to retain the stabilizing function of the interosseous ligament, thus avoiding the use of a fixation device. As illustrated in Figure 2, a bone defect measuring 15 mm in length was created by medio-diaphyseal osteotomy using a wireless battery oscillating saw (Acculan 3Ti, Aesculap, Germany). A physiological saline rinse was performed to remove bone debris. To avoid bone regeneration of the created defect by the periosteum of the radius, a bi-layer membrane of polylactic glycolic acid (PLGA, Tisseos®, Biomedical Tissues, Nantes, France) [46] was interposed between the radius and the BCP granules or the pre-vascularized synthetic graft. The segmental bone defect was either left empty, filled with BCP granules moistened with saline, or a vascularized synthetic graft produced in a subcutaneous site of the same rabbit (BCP + Pedicle or BCP + SVF + Pedicle). The surgical wound was closed in layers using resorbable sutures. As before, the operated animals were monitored daily to check their locomotion and proper cutaneous healing of the surgical site. After 8 weeks of implantation in bone defects, the animals were euthanized as previously described. The ulna was dissected and immediately fixed in buffered 10% formalin solution and stored at 4°C for μCT and histology analysis.

Injection of the radio-opaque vascular compound into rabbits

After 8 weeks of subcutaneous implantation, the first group of rabbits were sacrificed in order to study vascularization inside the chambers containing either the BCP, BCP + Pedicle or BCP + SVF + Pedicle. The animals were placed under general anesthesia as previously described and received a dose of heparin (50 IU/kg, Heparin Choay® 25000 IU/5 mL, Sanofi-Aventis) to reduce blood coagulation. The animals were immediately euthanized by intravenous injection of pentobarbital (1 ml / kg, Dolethal, Vetoquinol). After euthanasia, a medial skin incision in the abdominal region was performed. The dissection was performed to

expose the abdominal aorta, which was clamped and ligated proximally with a resorbable suture (Vycril® 3-0 coil, Ethicon, Johnson & Johnson, France). The aorta was catheterized with a silicone tube of similar diameter to inject a polymerizable silicone-based vascular contrast product containing lead (Microfil®, MV-122, Flow Tech Inc., Carver, MA, USA). The silicon tube was pre-filled with heparinized saline in order to avoid air bubbles using a peristaltic pump (Masterflex^{TM}, France). The radio-opaque solution (containing a yellow dye) was prepared according to the manufacturer's instructions. It consisted of 45% vol. MV-122, 50% vol. of the diluent solution and 5% vol. of the curing agent. The vascular contrast agent was perfused into the carotid artery using a peristaltic pump at a flow rate of 20 ml/min, corresponding to a physiological pressure of 100–120 mm Hg. Complete filling of the arteries and capillaries was assessed when the blood vessels appeared yellow. The vascular contrast agent was left to polymerize at room temperature for 30 min. The chambers were then dissected and immediately fixed in buffered 10% formalin solution and stored at 4°C for µCT and histology analysis.

Micro-computed tomography

Samples which were perfused with the contrast agent to demonstrate vasculature were characterized by high-resolution X-ray µCT (Skyscan uCT 1076, Kontich, Belgium) before and after decalcification. The acquisition was carried out at 50 kV over 180 ° with axial sections measuring 0.7 mm, giving a resolution of 18 µm / pixel. 3D reconstruction of the images was carried out using NRecon, Dataviewer, CTvox and CTan (Bruker, Skyscan) software. Given this spatial resolution, large vessel diameters as well as fine vasculature down to 50 µm can be observed and measured. The filling of the chambers with BCP was measured and expressed as material volume. The vascular volume was determined using the bone volume / total volume parameter (BV/TV) after decalcification of the samples.

Histology and immunohistochemistry

After fixation, the samples were decalcified in 4.13% ethylenediamine tetra acetic acid (EDTA)/0.2% paraformaldehyde in phosphate-buffered saline, pH 7.4 for 96 hours at 50°C using automated microwave decalcifying apparatus (KOS Histostation; Milestone Medical, Kalamazoo, Michigan, USA). The samples were then dehydrated in ascending series of ethanol baths (80, 95 and 100%) and finally in butanol for 30 minutes in an automated dehydration station (Microm Microtech, Lyon, France). The samples were then impregnated with liquid paraffin at 56°C (Histowax; Histolab, Gottenburg, Sweden) and embedded at −16°C. Blocks were cut using a standard microtome (Leica RM2255; Leica Biosystems, Nanterre, France). Thin histology sections (3 to 5 µm thick) were made radially for subcutis implants and longitudinally for ulnar defects. Sections were stained using the Masson trichrome technique in an automated coloration station (Microm Microtech). This staining combines hematoxylin for cell nuclei (blue/black), fuchsine for cytoplasm, muscle and erythrocytes (red), and light green solution for collagen (green). The stained slices were scanned (NanoZoomer; Hamamatsu, Photonics, Hamamatsu City, Shizuoka Prefecture, Japan) and observed and analyzed with a virtual microscope (NDP view; Hamamatsu). The number of blood vessels per area (presented as the number of blood vessel/mm^2) and the average vessel diameter were determined for the entire cross section of Masson Trichrome stained samples. Vascularization in the subcutis chambers was also identified with the anti-CD31 antibody which labels endothelial cells. Briefly, heat-mediated antigen retrieval was performed for 20 hours with Tris-EDTA (pH 9) at 60°C on deparaffinized sections. Quenching of endogenous peroxidase activity was mediated by 3% hydrogen peroxide incubation. Nonspecific binding sites were blocked with 5% goat serum, 1% bovine serum albumin (BSA) in Tris Buffered Saline 1X pH=7.4 Tween 0.05% (T.B.S., ScyTek Laboratories, Utah, USA). All washing steps were conducted using T.B.S. 1X pH=7.4 Tween

0.05%. Mouse monoclonal antibody to CD31/PECAM-1 (SPM122, M01513, Bosterbio) at a dilution of 1:25 was used, followed by incubation with a secondary goat anti-mouse antibody at a dilution of 1:100 (E0433, Dako, Denmark). The target antigen signal was amplified using streptavidin peroxidase (P0397, Dako, Denmark), revealed by diaminobenzidine (DAB). All sections were dehydrated and counterstained using Gill's hematoxylin and mounted using Pertex mounting medium. Sections were scanned (NanoZoomer; Hamamatsu, Photonics, Hamamatsu City, Shizuoka, Japan) and observed using a virtual microscope (NDP view; Hamamatsu).

Statistics

The data were expressed as an average ± standard deviation (SD). Analysis of the results of *in vivo* experiments was performed using the GraphPad Prism 6.0 software with a one-way ANOVA test. Tukey's multiple comparisons tests was conducted to assess statistical differences between the distinct groups. The significance threshold was set at $p \leq 0.05$.

Results

Preparation of SVF and multipotency of ATSCs

Approximately 6 g (5.8 ± 1.4 g) of adipose tissue was harvested and the SVF was prepared extemporaneously within 1 hour by mechanical disruption, enzyme digestion and centrifugation. The average number of nucleated cells in the prepared SVF was $3.57\ 10^5 \pm 1.24\ 10^5$ cells/ per mL after re-suspension in 1.5 mL of PBS and then the cell suspension was mixed with BCP granules. SVF was cultured *in vitro* and the constituent plastic adherent cells exhibited the tri-lineage characteristics typical of MSCs (Supplementary Figure 1). Briefly, in adipogenic differentiation conditions, lipid droplets were observed after staining with Red Oil. After osteogenic induction, the cells produced a mineralized collagen matrix, highlighted by Alizarin red staining. Cell pellets, cultured in the presence of chondrogenic differentiation

factors, showed the production of an extracellular matrix rich in glycosaminoglycans, as demonstrated by Alcian blue staining.

Characterizing the content of the subcutis implanted chambers

All rabbits survived the surgeries without complications, and had normal locomotion and weight bearing ability. After 8 weeks of subcutaneous implantation, all implants appeared well-integrated into the surrounding subcutis tissue, with no evidence of either rejection or necrosis. Vascular patency of the artery and vein passing through the chamber was observed for all pedicle implants (Figure 2a). The contents of the vascularized pedicle chambers exhibited good cohesion between the BCP granules due to abundant fibrosis (Figure 2b). In contrast, the BCP granules implanted without a pedicle appeared less compact after opening the chambers (Supplementary Figure 2). μCT showed that the BCP biomaterial granules had a cylindrical shape formed by the 3D printed PLGA chamber (Figure 3a-c). As shown in Figure 3g, the three groups had very comparable biomaterial filling percentages. After injecting the contrast agent and decalcifying the explants, it was possible to observe the vascular pedicle and new vasculature following 3D reconstruction of the μCT images. As shown in Figure 3d, the vascularization was negligible inside the chambers containing the BCP granules without a pedicle and was mainly located in the surrounding fibrous tissue capsule that had formed around the implantable chambers. Conversely, abundant vasculature with many small blood vessels was observed inside chambers containing BCP granules with a vascular pedicle (Figure 3e-f). Both the BCP + Pedicle and BCP + SVF + Pedicle groups exhibited abundant blood vessel branches that had grown from the pedicle (see supplementary video). For a more detailed view of samples, particularly for cross-sectional views before and after decalcification see Supplementary Figure 3. In Figure 3h, quantification of the μCT vascular volume data revealed a non-significantly trend towards higher vascular volume in the BCP +

Pedicle group (2.33 ± 1.50, n=5) and BCP + SVF + Pedicle group (1.82 ± 1.38, n=4) compared to the control BCP group without a pedicle (0.45 ± 0.34, n=3) (Figure 3h).

Histological Masson Trichrome images showed that the BCP granules were encapsulated in a dense collagen matrix for all three implant groups (Figure 4a). The pedicle implants appeared richer in collagen, with stronger fiber condensation, compared with the control BCP without a pedicle, however, bone tissue was not observed in any of the three implant groups. At higher magnification, giant nucleated cells were present in contact with the BCP biomaterial and were more prevalent in the BCP group without a pedicle. The vascular pedicles were clearly visible on the histological sections of the BCP + Pedicle and BCP + SVF + Pedicle groups. CD31 immunohistochemistry staining of endothelial cells are shown in Figure 4b surrounding the blood vessels and corroborate the structures observed by Masson Trichrome are indeed blood vessels. In Figure 4c, quantification of the number of blood vessel per area in Masson trichrome stained sections reveals no statistical difference between groups, however the average diameter (µm; excluding the diameter of the pedicle) of the blood vessels present was significantly greater ($p < 0.02$) for the BCP + Pedicle (21.98 ± 2.70, n=9) compared with the BCP alone group (17.83 ± 1.08, n=4). BCP + SVF + Pedicle (21.26 ± 1.94, n=6) was not statistically higher ($p<0.07$) compared with the BCP group alone. From both the histology and immumohistochemistry it is clear that the creation of a vascularized construct, through inclusion of a pedicle, stimulated angiogenesis, however the addition of SVF to the pedicle group had no observed benefit on vascularization.

Transplantation of pre-vascularized synthetic grafts enhanced bone healing in ulna defects in rabbits

After 8 weeks in subcutis sites, the pre-vascularized constructs were transplanted into a segmental critical-sized defect created at the mid-diaphyseal level of the ulna which was isolated from the radius using a PLGA membrane. Eight weeks after transplantation, the ulnas were characterized by µCT and histology. As shown in Figure 5, the ulna defect that was left

empty exhibited limited bone healing, proving that a critical-sized defect was created. The ulna defects filled with BCP granules had lower radio-opacity than those filled with the pre-vascularized grafts. MV+BV / TV (material volume + bone volume / total volume) measurements revealed significantly higher bone content in the pre-vascularized BCP + SVF + Pedicle grafts (37.65 ± 4.21, n=6) compared with the BCP group (23.73 ± 7.18, n=4), $p < 0.03$. BCP, BCP + Pedicle (34.53 ± 9.81, n=6), and BCP + SVF + Pedicle were all significantly higher compared to empty defects (4.82 ± 2.57, n=3), $p < 0.01$, $p < 0.0001$, and $p < 0.0001$ respectively. As illustrated in Figure 6, histological examination corroborated the µCT results. The empty defects remained unbridged. Ulna defects filled with BCP granules showed limited bone healing from the edges. Bone formation was observed within the defects that received the transplanted pre-vascularized synthetic constructs; however, some tissue necrosis was also observed. In both pre-vascularized constructs, new bone tissue was observed in contact with the BCP biomaterials.

Discussion

Bone is a highly vascularized tissue with bone cells residing within a 100-200 µm proximity to a blood vessel or capillary in order to ensure adequate supply of vital oxygen and nutrients. For this reason, when a biomaterial construct is not vascularized at the time of implantation, ischemia occurs, and high cell mortality is observed at the site. In the current study, implants were constructed by filling 3D-printed implantable chambers with BCP granules, a ceramic with proven bone-forming capabilities in pre-clinical and clinical trials [7,32,47]. The chamber held the granules in place, giving the construct a compact shape, while also making it easy to position the vascular pedicle. This pre-clinical study in rabbits demonstrates the feasibility of producing vascularized synthetic grafts in inguinal subcutaneous sites, and their capacity for bone healing after transplantation into a critical-sized bone defect.

There have been considerable advances in regenerative approaches aimed at overcoming the limitations of autologous bone grafting, however lack of adequate vascularization of synthetic grafts remains a major obstacle for reconstructing large bone defects. In the current study, we created a vascularized construct *in situ* by using an isolated pedicle composed of a peripheral artery and an adjacent vein, which were easily isolated from the surrounding tissues and passed through the implantable chamber. This achieved extensive neo vascularization with blood vessels sprouting from the central vasculature following subcutaneous implantation compared to the BCP group without a pedicle. Specifically, increased vessel size was revealed by histological analysis after 8 weeks, in line with increased vascular volume observed by μCT. This finding is in agreement with previous studies demonstrating the enhancement of neovascularization by using a vascular pedicle in unison with synthetic biomaterials [48]. Furthermore, this technique has advantages over previous *in situ* vascularized biomaterial constructs made using AV loops as it overcame the laborious stage of microsurgical anastomosis [49].

We confirmed that the autologous rabbit SVF contained multilineage-potential MSCs, similar to those derived from human adipose tissue [33]. We did not investigate the fate of transplanted cells contained in SVF, in particular ATSCs, because it was an autologous model, however it is generally considered that most transplanted MSCs do not engraft and their therapeutic effect is via paracrine mechanisms [50,51]. The delivery of SVF to the pedicle construct did not enhance vascularization further than the use of a pedicle alone. This may be because the number of cells present in the SVF would be minute in comparison to those delivered by the pedicle which induced vascularization to such a degree that any increase by SVF was negligible. To distinguish if SVF alone has a beneficial effect on vascularization as observed by previous studies [52], an additional group containing only BCP + SVF would be required, however this is out of the scope of the current study as the

focus was primarily to use a pedicle to achieve pre-vascularization, and secondly to determine if SVF would enhance this further.

While pre-vascularized constructs were successfully achieved by using our approach, there was an absence of bone formation in the subcutis constructs following implantation for 8 weeks. This is in contrast to a recent study which observed bone formation using SVF in a similar vascular pedicle approach [2], with differences possibly caused by the much lower cell number used in the current study. However, the bone induction observed by Epple et al was likely due to another aspect of their construct since the SVF showed no increase in bone formation compared to other groups without SVF, it could also be due to the longer implantation time of 12 weeks in contrast to the 8 week period employed here. We have previously observed that cultured expanded MSCs derived from adipose tissue significantly enhanced neovascularization *in vivo* but failed to induce *de novo* bone in subcutis sites [40], in agreement with our present results. A comparable study encompassing a vascular pedicle, albeit just the vein, passing centrally through a 3D printed calcium phosphate scaffold has recently been reported [53]. Autologous bone marrow was placed in unison with the biomaterial around the femoral vein of rats in subcutaneous site for 8 weeks. Contrary to our study, newly formed bone tissue was observed in the explants loaded with bone marrow aspirates [53]. Together, this suggests the superiority of employing bone marrow rather than SVF, whilst still permitting delivery in a single surgery. While promising, these studies have not assessed the bone regeneration potential of the pre-vascularized constructs in bone defects. The current study represents the first evaluation of this type of *in situ* vascularized construct in a bone defect. Autologous transplantation of this vascularized synthetic graft into a rabbit ulna bone defect was possible without tissue morbidity and furthermore, after 8 weeks, μCT and histological examination showed good bone integration of the synthetic pre-vascularized graft and bone defect healing. The addition of SVF yielded no benefit in terms of

bone formation compared with the pedicle group without SVF, perhaps since both constructs were equally well vascularized upon transplantation to the bone defect.

Some limitations of the current study include firstly, since the granules of the BCP group often fell apart upon opening of the chambers, in contrast to the pedicle groups where firm constructs in the shape of the chambers were formed, this dictated that fresh BCP granules were used for the BCP control group in the bone defect surgery rather than those that had been implanted subcutaneously 8 weeks prior, as was the case for the two pedicle groups. It must also be noted that while our prevascularized construct approach circumvents issues of autologous bone graft harvesting and tissue availability, it required two surgeries and an 8-week preparation time for prevascularization, which is incompatible with severe and urgent trauma. Furthermore, the creation of the ulna defects was not standardized, which may have contributed to some non-unions at the extremity of the defects (Figure 5a) which may be overcome by the use of surgical guides customized to the skeletal anatomy [54]. In addition, the prevascularized construct was transplanted into the ulna defect without anastomosis to the local vasculature. The limited size of the rabbit model and the availability of a suitable local vasculature to connect the transplant prevented us from performing anastomoses. This may be responsible for the small quantity of necrosis observed within these constructs after transplantation into the bone defects, nevertheless, new bone tissue was formed, and significant defect healing was observed. Finally, we did not conduct mechanical testing of the bone constructs which would have evaluated the functional strength of the implants and given a more precise view of the integrity of the bone tissue that was formed. While calcium phosphate biomaterials, such as the BCP used in the current study, have proven osteoconductive properties, they have very low mechanical properties in comparison with those of native bone tissue and it will thus undoubtedly be necessary to provide them with mechanical reinforcement until adequate bone formation has occurred. A mechanically

suitable, vascularized construct has the potential to ensure effective bone healing of large bone defects. The current study has described a technique to produce a simple, fast and reproducible pre-vascularized bone construct, and presents the potential of overcoming the disadvantages of autologous grafting.

Conclusion

This study has demonstrated the feasibility of *in situ* fabrication of vascularized synthetic grafts in an ectopic site using a vascular pedicle passing through the biomaterial. After inguinal subcutaneous implantation, all the pedicle implants exhibited adequate vascular permeability, and sprouting of a vascular network. The transplantation of the pre-vascularized synthetic bone grafts into critical-sized ulnar defects led to significantly higher bone regeneration compared to the transplantation of the BCP biomaterial without a pedicle. This surgical technique was simple, fast and reproducible, and offers the possibility to preserve bone stock and overcome the limitations of autologous grafting.

Acknowledgments

This work was financially supported by a grant from the European Commission: ORTHOUNION (#773288). The patients' association 'Ligue Française contre les neurofibromatoses' is greatly acknowledged for supporting the PhD thesis of Luciano Vidal. Meadhbh Brennan is supported by the Marie Skłodowska Curie Individual Fellowship PARAGEN H2020-MSCA-IF-2015-708711. We appreciate the technical assistance of Clémence, Thébaud, and Jérôme Amiaud for preparation of the SVF and for histology, respectively. We also acknowledge the staff of the CRIP platform at the Veterinary school for the care, anesthesia and post-operative treatment of the animals.

Data availability

The raw/processed data required to reproduce these findings can be accessed by contacting the authors directly.

References

[1] L. Vidal, C. Kampleitner, M.Á. Brennan, A. Hoornaert, P. Layrolle, Reconstruction of Large Skeletal Defects: Current Clinical Therapeutic Strategies and Future Directions Using 3D Printing, Front Bioeng Biotechnol. 8 (2020) 61. https://doi.org/10.3389/fbioe.2020.00061.

[2] C. Epple, A. Haumer, T. Ismail, A. Lunger, A. Scherberich, D.J. Schaefer, I. Martin, Prefabrication of a large pedicled bone graft by engineering the germ for de novo vascularization and osteoinduction, Biomaterials. 192 (2019) 118–127. https://doi.org/10.1016/j.biomaterials.2018.11.008.

[3] G. Merlino, M. Borsetti, M. Boltri, Reverse radial artery bone flap reconstruction of segmental metacarpal losses, J Hand Surg Eur Vol. 32 (2007) 98–101. https://doi.org/10.1016/j.jhsb.2006.08.015.

[4] J.B. Moore, J.M. Mazur, D. Zehr, P.K. Davis, E.G. Zook, A biomechanical comparison of vascularized and conventional autogenous bone grafts, Plast. Reconstr. Surg. 73 (1984) 382–386.

[5] J.E. Lipa, C.B. Novak, P.A. Binhammer, Patient-reported donor-site morbidity following anterolateral thigh free flaps, J Reconstr Microsurg. 21 (2005) 365–370. https://doi.org/10.1055/s-2005-915203.

[6] M.Á. Brennan, A. Renaud, J. Amiaud, M.T. Rojewski, H. Schrezenmeier, D. Heymann, V. Trichet, P. Layrolle, Pre-clinical studies of bone regeneration with human bone marrow stromal cells and biphasic calcium phosphate, Stem Cell Res Ther. 5 (2014). https://doi.org/10.1186/scrt504.

[7] A.-L. Gamblin, M.A. Brennan, A. Renaud, H. Yagita, F. Lézot, D. Heymann, V. Trichet, P. Layrolle, Bone tissue formation with human mesenchymal stem cells and biphasic calcium phosphate ceramics: the local implication of osteoclasts and macrophages, Biomaterials. 35 (2014) 9660–9667. https://doi.org/10.1016/j.biomaterials.2014.08.018.

[8] M.H. Mankani, S.A. Kuznetsov, P.G. Robey, Formation of hematopoietic territories and bone by transplanted human bone marrow stromal cells requires a critical cell density, Exp. Hematol. 35 (2007) 995–1004.

[9] M.H. Mankani, S.A. Kuznetsov, R.M. Wolfe, G.W. Marshall, P.G. Robey, In vivo bone formation by human bone marrow stromal cells: reconstruction of the mouse calvarium and mandible, Stem Cells. 24 (2006) 2140–2149. https://doi.org/10.1634/stemcells.2005-0567.

[10] M.A. Brennan, J.-M. Davaine, P. Layrolle, Pre-vascularization of bone tissue-engineered constructs, Stem Cell Res Ther. 4 (2013) 96. https://doi.org/10.1186/scrt307.

[11] J. Marler, J. Upton, R. Langer, J. Vacanti, Transplantation of cells in matrices for tissue regeneration, Adv. Drug Deliv. Rev. 33 (1998) 165–182.

[12] N.B. Thébaud, R. Siadous, R. Bareille, M. Remy, R. Daculsi, J. Amédée, L. Bordenave, Whatever their differentiation status, human progenitor derived - or mature - endothelial cells induce osteoblastic differentiation of bone marrow stromal cells, J Tissue Eng Regen Med. 6 (2012) e51-60. https://doi.org/10.1002/term.1539.

[13] M. Maisani, D. Pezzoli, O. Chassande, D. Mantovani, Cellularizing hydrogel-based scaffolds to repair bone tissue: How to create a physiologically relevant micro-environment?, J Tissue Eng. 8 (2017). https://doi.org/10.1177/2041731417712073.

[14] X. Liu, W. Chen, C. Zhang, W. Thein-Han, K. Hu, M.A. Reynolds, C. Bao, P. Wang, L. Zhao, H.H.K. Xu, Co-Seeding Human Endothelial Cells with Human-Induced Pluripotent Stem Cell-Derived Mesenchymal Stem Cells on Calcium Phosphate Scaffold Enhances Osteogenesis and Vascularization in Rats, Tissue Eng Part A. 23 (2017) 546–555. https://doi.org/10.1089/ten.tea.2016.0485.
[15] S.V. Murphy, A. Atala, 3D bioprinting of tissues and organs, Nat. Biotechnol. 32 (2014) 773–785. https://doi.org/10.1038/nbt.2958.
[16] D.B. Kolesky, K.A. Homan, M.A. Skylar-Scott, J.A. Lewis, Three-dimensional bioprinting of thick vascularized tissues, Proc Natl Acad Sci U S A. 113 (2016) 3179–3184. https://doi.org/10.1073/pnas.1521342113.
[17] H.-W. Kang, S.J. Lee, I.K. Ko, C. Kengla, J.J. Yoo, A. Atala, A 3D bioprinting system to produce human-scale tissue constructs with structural integrity, Nat. Biotechnol. 34 (2016) 312–319. https://doi.org/10.1038/nbt.3413.
[18] R.K. Khouri, B. Koudsi, H. Reddi, Tissue transformation into bone in vivo. A potential practical application, JAMA. 266 (1991) 1953–1955.
[19] A. Kaempfen, A. Todorov, S. Güven, R.D. Largo, C. Jaquiéry, A. Scherberich, I. Martin, D.J. Schaefer, Engraftment of Prevascularized, Tissue Engineered Constructs in a Novel Rabbit Segmental Bone Defect Model, Int J Mol Sci. 16 (2015) 12616–12630. https://doi.org/10.3390/ijms160612616.
[20] P.H. Warnke, J. Wiltfang, I. Springer, Y. Acil, H. Bolte, M. Kosmahl, P.A.J. Russo, E. Sherry, U. Lützen, S. Wolfart, H. Terheyden, Man as living bioreactor: fate of an exogenously prepared customized tissue-engineered mandible, Biomaterials. 27 (2006) 3163–3167. https://doi.org/10.1016/j.biomaterials.2006.01.050.
[21] K. Mesimäki, B. Lindroos, J. Törnwall, J. Mauno, C. Lindqvist, R. Kontio, S. Miettinen, R. Suuronen, Novel maxillary reconstruction with ectopic bone formation by GMP adipose stem cells, Int J Oral Maxillofac Surg. 38 (2009) 201–209. https://doi.org/10.1016/j.ijom.2009.01.001.
[22] J.P. Beier, R.E. Horch, A. Arkudas, E. Polykandriotis, O. Bleiziffer, E. Adamek, A. Hess, U. Kneser, De novo generation of axially vascularized tissue in a large animal model, Microsurgery. 29 (2009) 42–51. https://doi.org/10.1002/micr.20564.
[23] Q. Dong, C. Lin, H. Shang, W. Wu, F. Chen, X. Ji, Y. Liu, J. Zhang, T. Mao, Modified approach to construct a vascularized coral bone in rabbit using an arteriovenous loop, J Reconstr Microsurg. 26 (2010) 95–102. https://doi.org/10.1055/s-0029-1243293.
[24] A.M. Boos, J.S. Loew, A. Weigand, G. Deschler, D. Klumpp, A. Arkudas, O. Bleiziffer, H. Gulle, U. Kneser, R.E. Horch, J.P. Beier, Engineering axially vascularized bone in the sheep arteriovenous-loop model, Journal of Tissue Engineering and Regenerative Medicine. 7 (2013) 654–664. https://doi.org/10.1002/term.1457.
[25] A. Arkudas, A. Lipp, G. Buehrer, I. Arnold, D. Dafinova, A. Brandl, J.P. Beier, C. Körner, S. Lyer, C. Alexiou, U. Kneser, R.E. Horch, Pedicled Transplantation of Axially Vascularized Bone Constructs in a Critical Size Femoral Defect, Tissue Eng Part A. 24 (2018) 479–492. https://doi.org/10.1089/ten.TEA.2017.0110.
[26] E. Polykandriotis, A. Arkudas, R.E. Horch, M. Stürzl, U. Kneser, Autonomously vascularized cellular constructs in tissue engineering: opening a new perspective for biomedical science, Journal of Cellular and Molecular Medicine. 11 (2007) 6–20. https://doi.org/10.1111/j.1582-4934.2007.00012.x.
[27] H. Kokemueller, S. Spalthoff, M. Nolff, F. Tavassol, H. Essig, C. Stuehmer, K.-H. Bormann, M. Rücker, N.-C. Gellrich, Prefabrication of vascularized bioartificial bone grafts in vivo

for segmental mandibular reconstruction: experimental pilot study in sheep and first clinical application, International Journal of Oral and Maxillofacial Surgery. 39 (2010) 379–387. https://doi.org/10.1016/j.ijom.2010.01.010.
[28] G.E. Holt, J.L. Halpern, C.C. Lynch, C.J. Devin, H.S. Schwartz, Imaging Analysis of the In vivo Bioreactor: A Preliminary Study, Clin Orthop Relat Res. 466 (2008) 1890–1896. https://doi.org/10.1007/s11999-008-0295-3.
[29] D. Han, X. Guan, J. Wang, J. Wei, Q. Li, Rabbit Tibial Periosteum and Saphenous Arteriovenous Vascular Bundle as an In Vivo Bioreactor to Construct Vascularized Tissue-Engineered Bone: A Feasibility Study, Artificial Organs. 38 (2014) 167–174. https://doi.org/10.1111/aor.12124.
[30] X. Wu, Q. Wang, N. Kang, J. Wu, C. Gu, J. Bi, T. Lv, F. Xie, J. Hu, X. Liu, Y. Cao, R. Xiao, The effects of different vascular carrier patterns on the angiogenesis and osteogenesis of BMSC-TCP-based tissue-engineered bone in beagle dogs, J Tissue Eng Regen Med. 11 (2017) 542–552. https://doi.org/10.1002/term.2076.
[31] C. Gjerde, K. Mustafa, S. Hellem, M. Rojewski, H. Gjengedal, M.A. Yassin, X. Feng, S. Skaale, T. Berge, A. Rosen, X.-Q. Shi, A.B. Ahmed, B.T. Gjertsen, H. Schrezenmeier, P. Layrolle, Cell therapy induced regeneration of severely atrophied mandibular bone in a clinical trial, Stem Cell Res Ther. 9 (2018). https://doi.org/10.1186/s13287-018-0951-9.
[32] E. Gómez-Barrena, P. Rosset, F. Gebhard, P. Hernigou, N. Baldini, H. Rouard, L. Sensebé, R.M. Gonzalo-Daganzo, R. Giordano, N. Padilla-Eguiluz, E. García-Rey, J. Cordero-Ampuero, J.C. Rubio-Suárez, J. Stanovici, C. Ehrnthaller, M. Huber-Lang, C.H. Flouzat-Lachaniette, N. Chevallier, D.M. Donati, G. Ciapetti, S. Fleury, M.-N. Fernandez, J.-R. Cabrera, C. Avendaño-Solá, T. Montemurro, C. Panaitescu, E. Veronesi, M.T. Rojewski, R. Lotfi, M. Dominici, H. Schrezenmeier, P. Layrolle, Feasibility and safety of treating non-unions in tibia, femur and humerus with autologous, expanded, bone marrow-derived mesenchymal stromal cells associated with biphasic calcium phosphate biomaterials in a multicentric, non-comparative trial, Biomaterials. 196 (2019) 100–108. https://doi.org/10.1016/j.biomaterials.2018.03.033.
[33] P.A. Zuk, M. Zhu, H. Mizuno, J. Huang, J.W. Futrell, A.J. Katz, P. Benhaim, H.P. Lorenz, M.H. Hedrick, Multilineage cells from human adipose tissue: implications for cell-based therapies, Tissue Eng. 7 (2001) 211–228. https://doi.org/10.1089/107632701300062859.
[34] V.M. Ramakrishnan, N.L. Boyd, The Adipose Stromal Vascular Fraction as a Complex Cellular Source for Tissue Engineering Applications, Tissue Eng Part B Rev. 24 (2018) 289–299. https://doi.org/10.1089/ten.TEB.2017.0061.
[35] J. Wang, Y. Liao, J. Xia, Z. Wang, X. Mo, J. Feng, Y. He, X. Chen, Y. Li, F. Lu, J. Cai, Mechanical micronization of lipoaspirates for the treatment of hypertrophic scars, Stem Cell Res Ther. 10 (2019). https://doi.org/10.1186/s13287-019-1140-1.
[36] G. Desando, I. Bartolotti, L. Martini, G. Giavaresi, N. Nicoli Aldini, M. Fini, A. Roffi, F. Perdisa, G. Filardo, E. Kon, B. Grigolo, Regenerative Features of Adipose Tissue for Osteoarthritis Treatment in a Rabbit Model: Enzymatic Digestion Versus Mechanical Disruption, Int J Mol Sci. 20 (2019). https://doi.org/10.3390/ijms20112636.
[37] C. Hao, S. Shintani, Y. Shimizu, K. Kondo, M. Ishii, H. Wu, T. Murohara, Therapeutic angiogenesis by autologous adipose-derived regenerative cells: comparison with bone marrow mononuclear cells, Am. J. Physiol. Heart Circ. Physiol. 307 (2014) H869-879. https://doi.org/10.1152/ajpheart.00310.2014.

[38] M. Behfar, F. Sarrafzadeh-Rezaei, R. Hobbenaghi, N. Delirezh, B. Dalir-Naghadeh, Adipose derived stromal vascular fraction improves early tendon healing: an experimental study in rabbits, Veterinary Research Forum. 2 (2011) 248–253.
[39] M. Mazo, S. Hernández, J.J. Gavira, G. Abizanda, M. Araña, T. López-Martínez, C. Moreno, J. Merino, A. Martino-Rodríguez, A. Uixeira, J.A. García de Jalón, J. Pastrana, D. Martínez-Caro, F. Prósper, Treatment of reperfused ischemia with adipose-derived stem cells in a preclinical Swine model of myocardial infarction, Cell Transplant. 21 (2012) 2723–2733. https://doi.org/10.3727/096368912X638847.
[40] M.A. Brennan, A. Renaud, F. Guilloton, M. Mebarki, V. Trichet, L. Sensebé, F. Deschaseaux, N. Chevallier, P. Layrolle, Inferior In Vivo Osteogenesis and Superior Angiogeneis of Human Adipose Tissue: A Comparison with Bone Marrow-Derived Stromal Stem Cells Cultured in Xeno-Free Conditions, Stem Cells Transl Med. 6 (2017) 2160–2172. https://doi.org/10.1002/sctm.17-0133.
[41] T. Murohara, Autologous adipose tissue as a new source of progenitor cells for therapeutic angiogenesis, J Cardiol. 53 (2009) 155–163. https://doi.org/10.1016/j.jjcc.2009.01.003.
[42] J. Zhou, H. Lin, T. Fang, X. Li, W. Dai, T. Uemura, J. Dong, The repair of large segmental bone defects in the rabbit with vascularized tissue engineered bone, Biomaterials. 31 (2010) 1171–1179. https://doi.org/10.1016/j.biomaterials.2009.10.043.
[43] R.M. El Backly, D. Chiapale, A. Muraglia, G. Tromba, C. Ottonello, F. Santolini, R. Cancedda, M. Mastrogiacomo, A modified rabbit ulna defect model for evaluating periosteal substitutes in bone engineering: a pilot study, Front Bioeng Biotechnol. 2 (2014) 80. https://doi.org/10.3389/fbioe.2014.00080.
[44] C. Wan, Q. He, G. Li, Allogenic peripheral blood derived mesenchymal stem cells (MSCs) enhance bone regeneration in rabbit ulna critical-sized bone defect model, J. Orthop. Res. 24 (2006) 610–618. https://doi.org/10.1002/jor.20119.
[45] T. Cordonnier, A. Langonné, P. Corre, A. Renaud, L. Sensebé, P. Rosset, P. Layrolle, J. Sohier, Osteoblastic differentiation and potent osteogenicity of three-dimensional hBMSC-BCP particle constructs, J Tissue Eng Regen Med. 8 (2014) 364–376. https://doi.org/10.1002/term.1529.
[46] A. Hoornaert, C. d'Arros, M.-F. Heymann, P. Layrolle, Biocompatibility, resorption and biofunctionality of a new synthetic biodegradable membrane for guided bone regeneration, Biomed Mater. 11 (2016) 045012. https://doi.org/10.1088/1748-6041/11/4/045012.
[47] P. Humbert, M.Á. Brennan, N. Davison, P. Rosset, V. Trichet, F. Blanchard, P. Layrolle, Immune Modulation by Transplanted Calcium Phosphate Biomaterials and Human Mesenchymal Stromal Cells in Bone Regeneration, Front Immunol. 10 (2019) 663. https://doi.org/10.3389/fimmu.2019.00663.
[48] P. Yang, X. Huang, J. Shen, C. Wang, X. Dang, H. Mankin, Z. Duan, K. Wang, Development of a new pre-vascularized tissue-engineered construct using pre-differentiated rADSCs, arteriovenous vascular bundle and porous nano-hydroxyapatide-polyamide 66 scaffold, BMC Musculoskelet Disord. 14 (2013) 318. https://doi.org/10.1186/1471-2474-14-318.
[49] J.P. Beier, R.E. Horch, A. Hess, A. Arkudas, J. Heinrich, J. Loew, H. Gulle, E. Polykandriotis, O. Bleiziffer, U. Kneser, Axial vascularization of a large volume calcium phosphate ceramic bone substitute in the sheep AV loop model, J Tissue Eng Regen Med. 4 (2010) 216–223. https://doi.org/10.1002/term.229.

[50] M.Á. Brennan, P. Layrolle, D.J. Mooney, Biomaterials Functionalized with MSC Secreted Extracellular Vesicles and Soluble Factors for Tissue Regeneration, Advanced Functional Materials. n/a (2020) 1909125. https://doi.org/10.1002/adfm.201909125.
[51] O.P.B. Wiklander, M.Á. Brennan, J. Lötvall, X.O. Breakefield, S. El Andaloussi, Advances in therapeutic applications of extracellular vesicles, Sci Transl Med. 11 (2019). https://doi.org/10.1126/scitranslmed.aav8521.
[52] E. Farré-Guasch, N. Bravenboer, M.N. Helder, E.A.J.M. Schulten, C.M. Ten Bruggenkate, J. Klein-Nulend, Blood Vessel Formation and Bone Regeneration Potential of the Stromal Vascular Fraction Seeded on a Calcium Phosphate Scaffold in the Human Maxillary Sinus Floor Elevation Model, Materials (Basel). 11 (2018). https://doi.org/10.3390/ma11010161.
[53] B. Charbonnier, A. Baradaran, D. Sato, O. Alghamdi, Z. Zhang, Y.-L. Zhang, U. Gbureck, M. Gilardino, E. Harvey, N. Makhoul, J. Barralet, Material-Induced Venosome-Supported Bone Tubes, Advanced Science. 0 (n.d.) 1900844. https://doi.org/10.1002/advs.201900844.
[54] L. Vidal, C. Kampleitner, S. Krissian, M.Á. Brennan, O. Hoffmann, Y. Raymond, Y. Maazouz, M.-P. Ginebra, P. Rosset, P. Layrolle, Regeneration of segmental defects in metatarsus of sheep with vascularized and customized 3D-printed calcium phosphate scaffolds, Sci Rep. 10 (2020) 7068. https://doi.org/10.1038/s41598-020-63742-w.

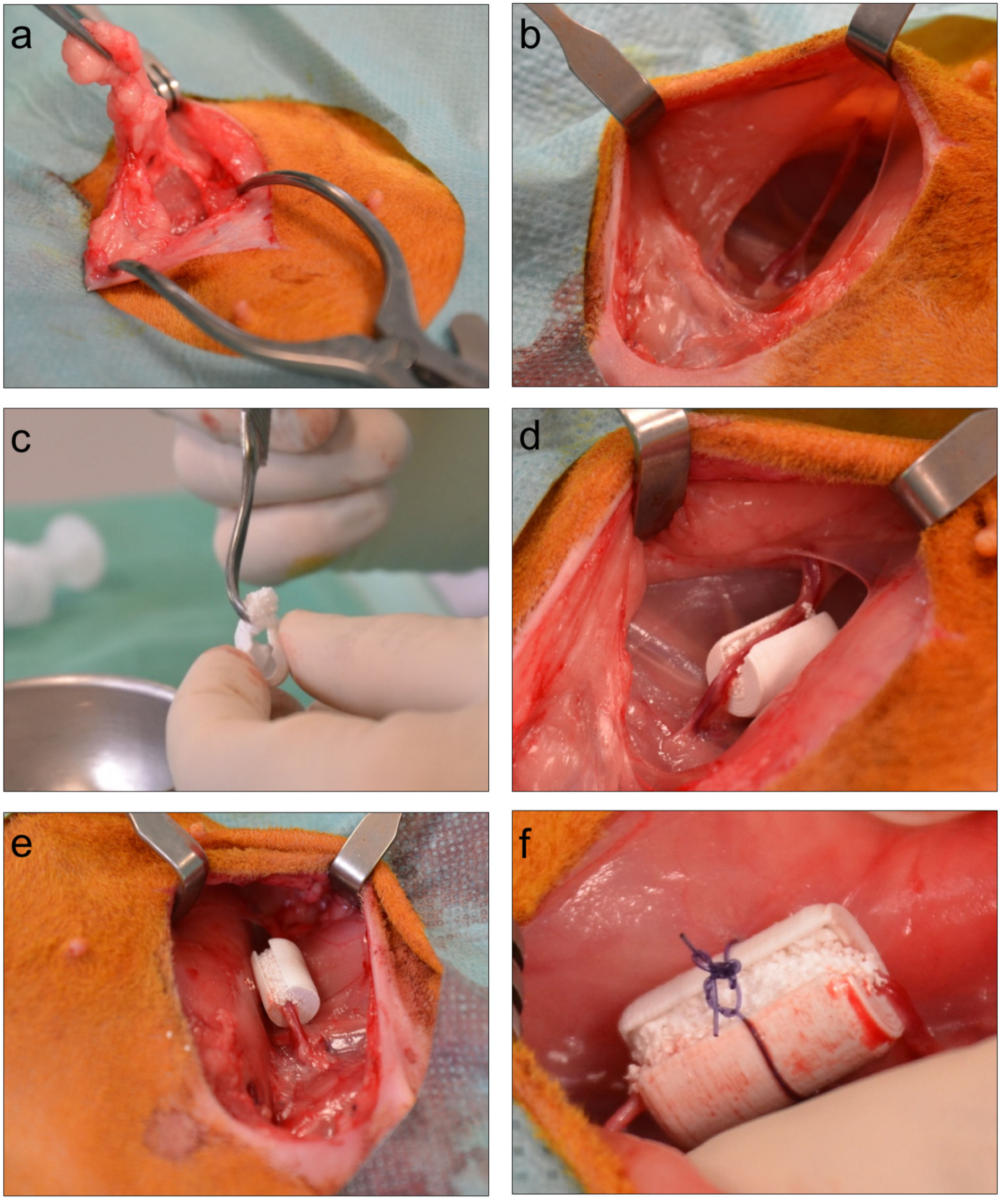
a
b
c
d
e
f


a


b


c

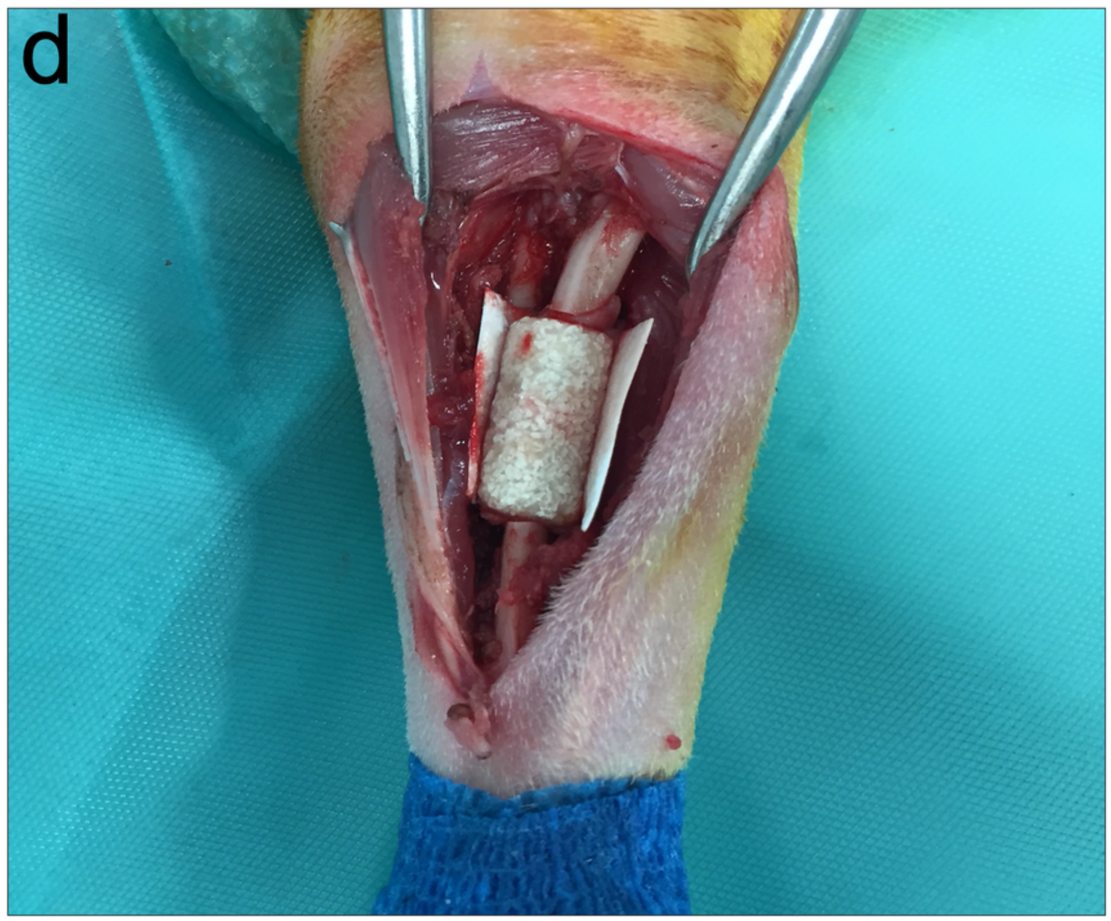
d

BCP

BCP + Pedicle

BCP + SVF + Pedicle

a

b

c

1mm

d

e

f

1mm

g

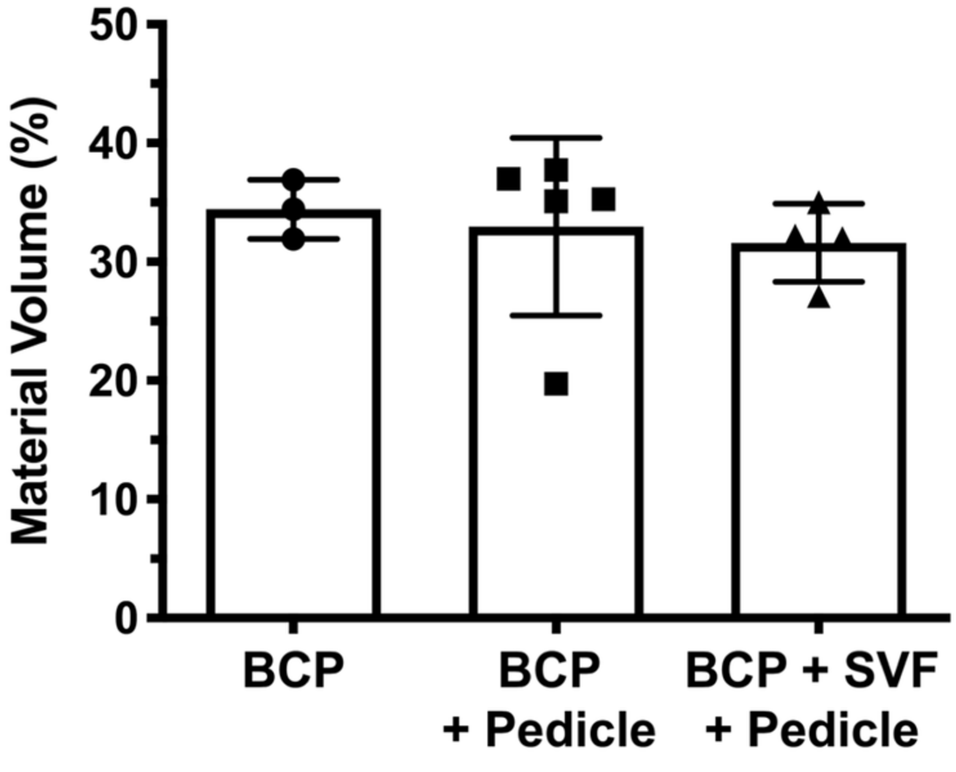

h

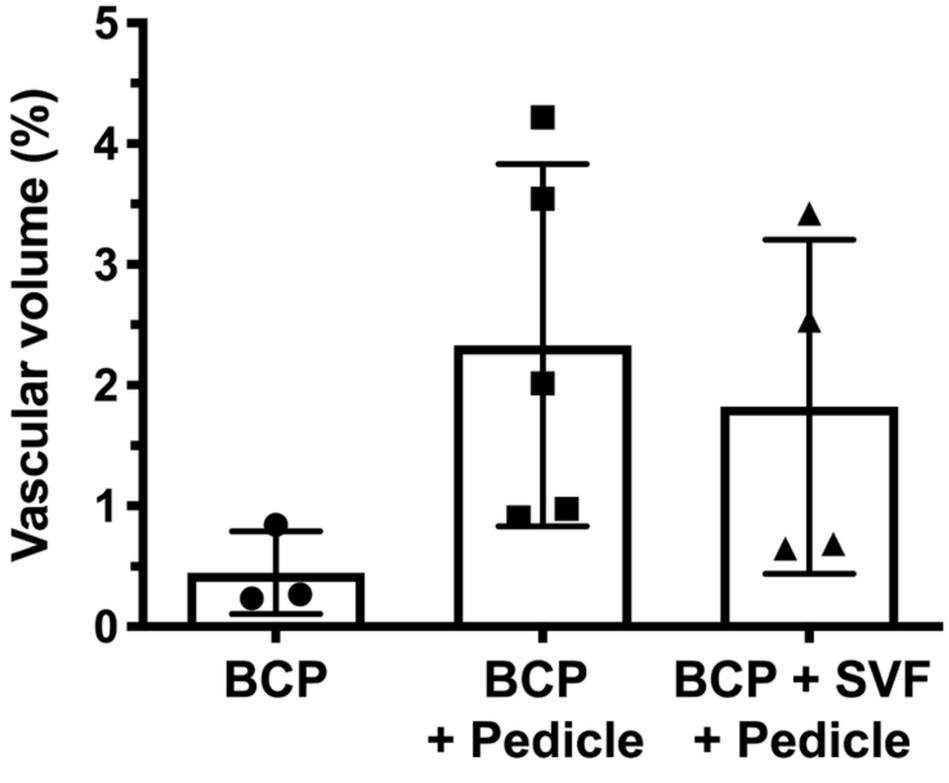

a

BCP

BCP + Pedicle

BCP + SVF + Pedicle

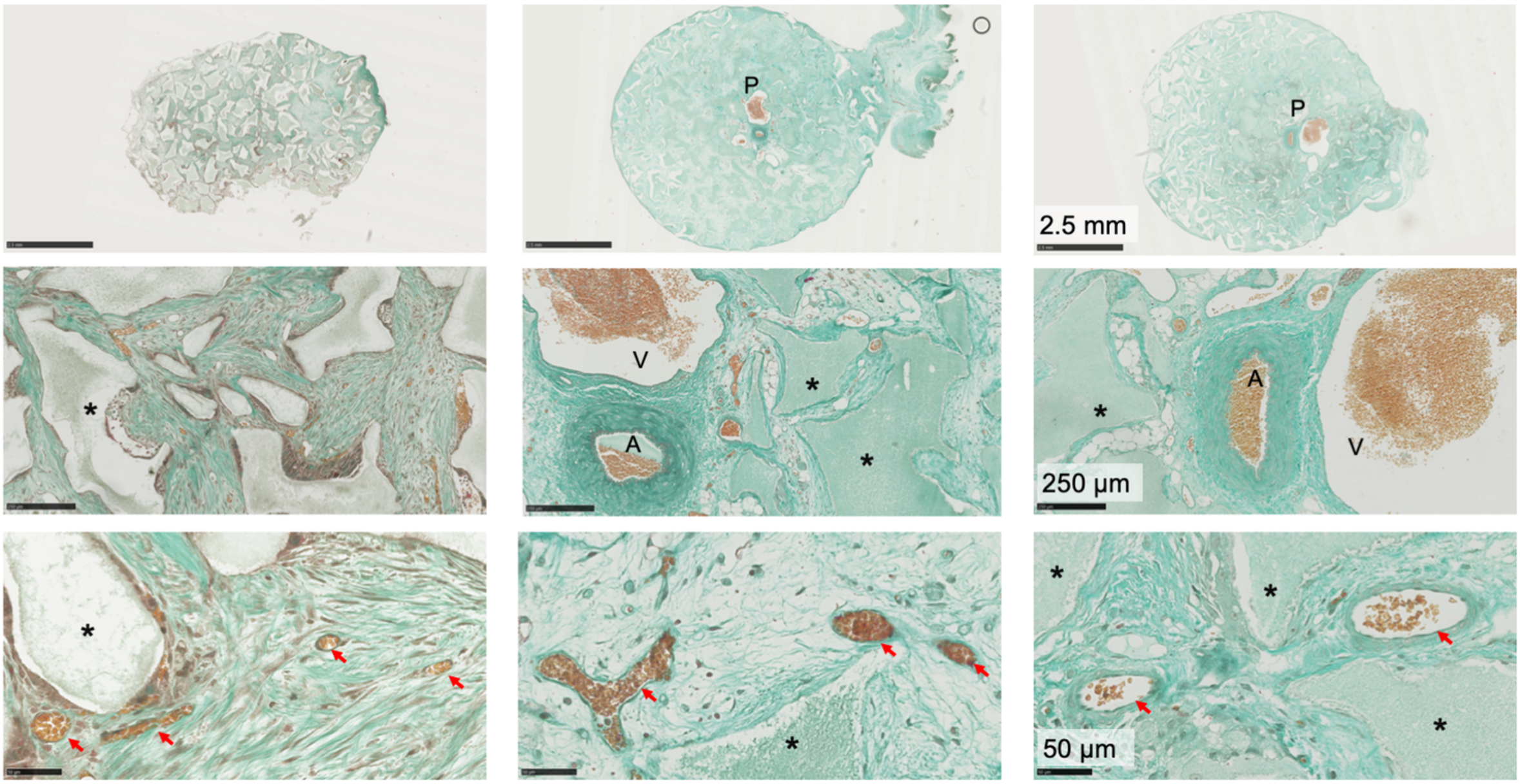

b

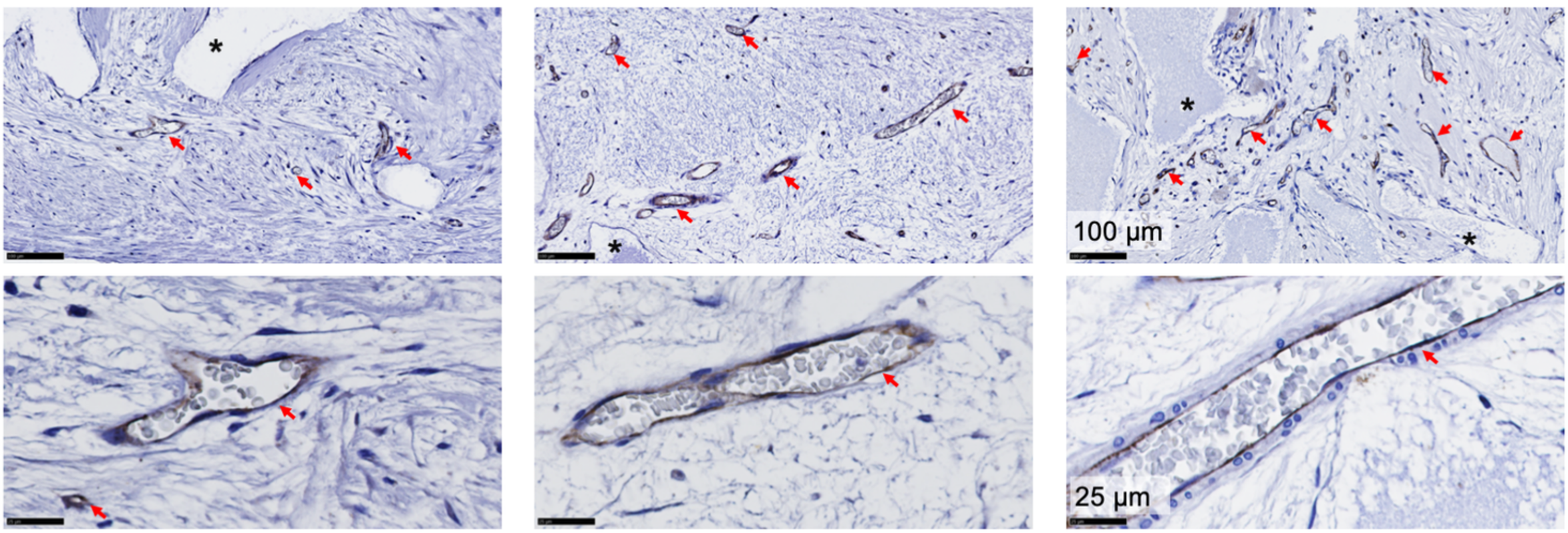

C

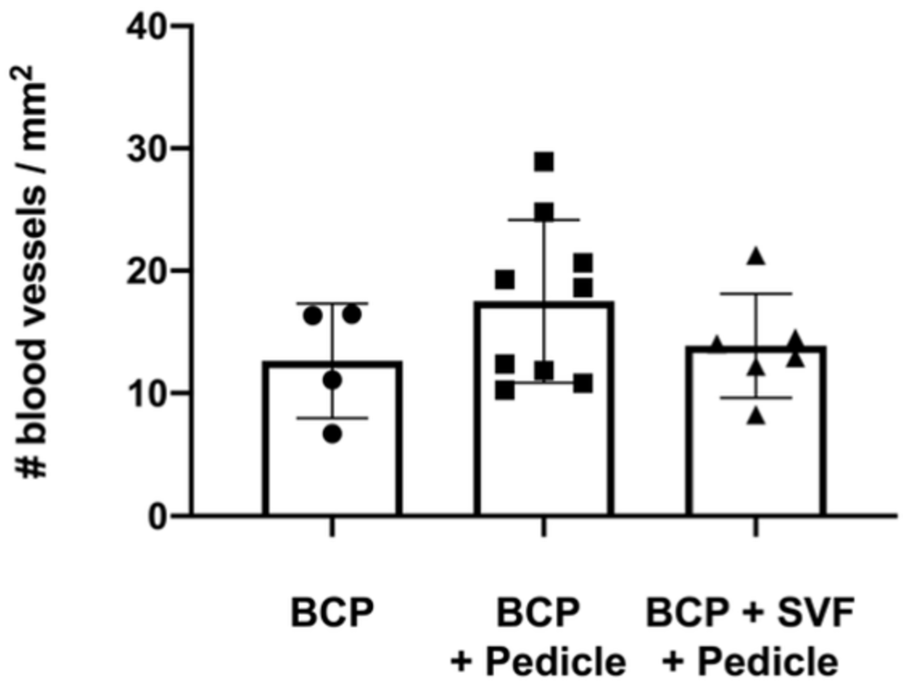

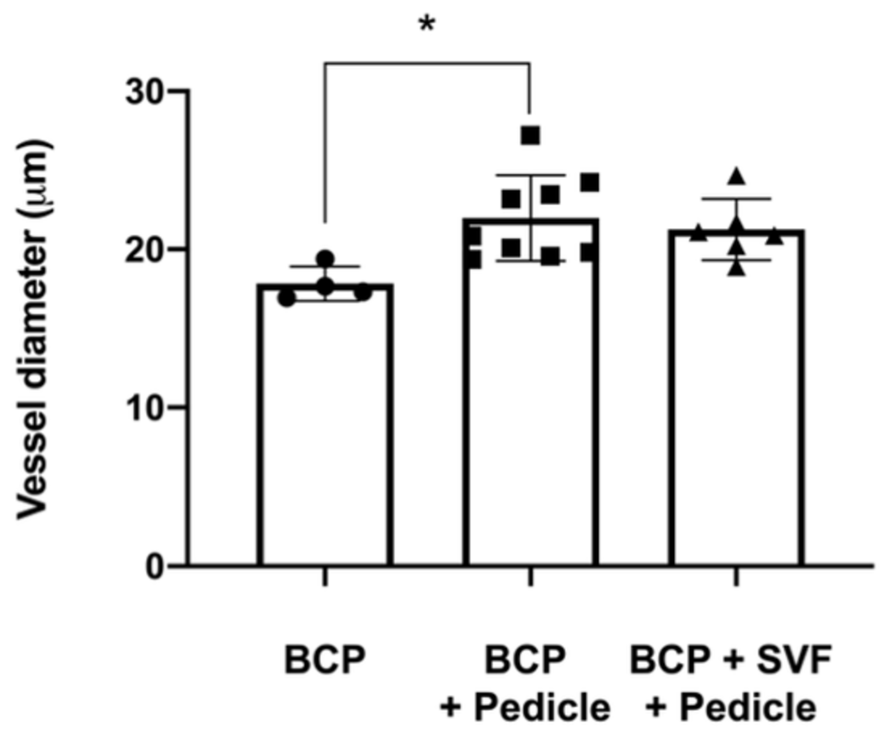

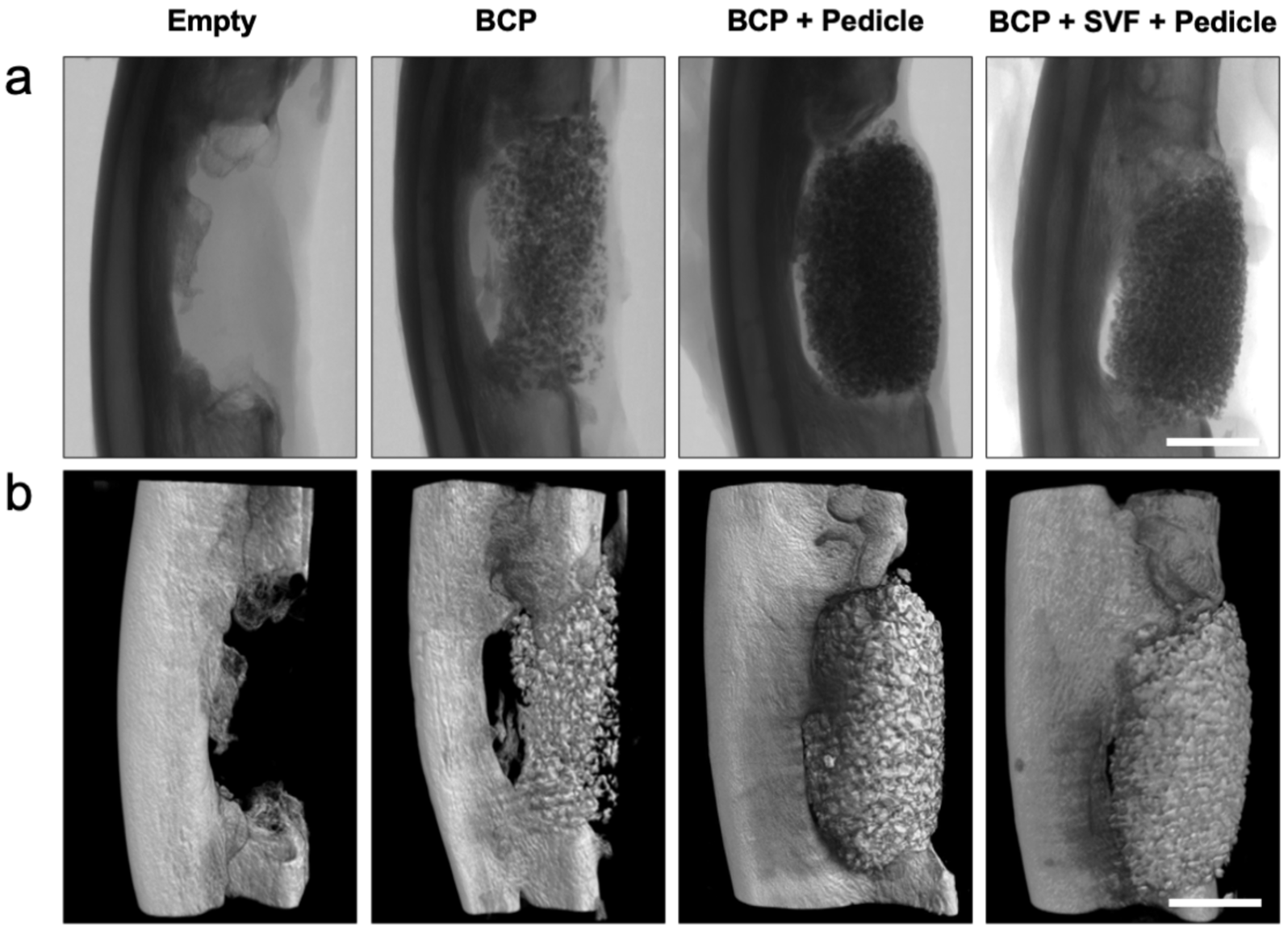
Empty
BCP
BCP + Pedicle
BCP + SVF + Pedicle
a
b

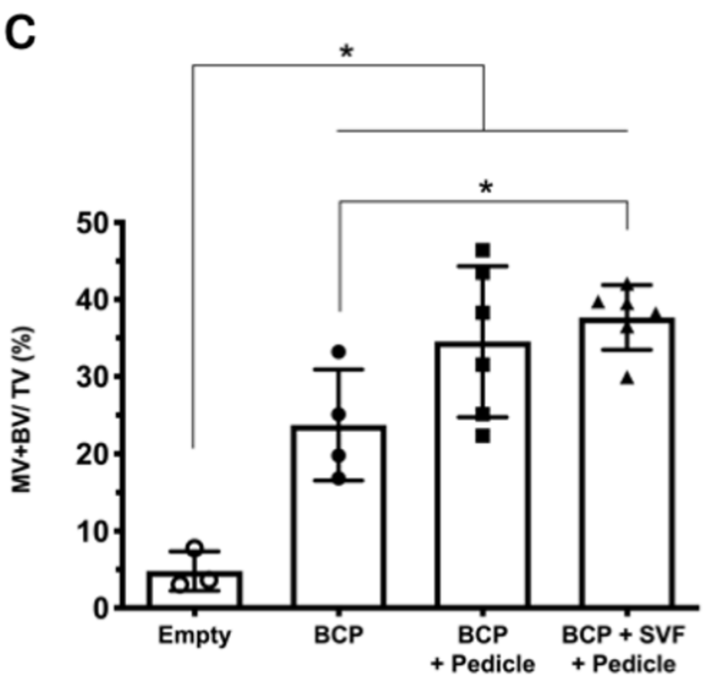
c
*
*
MV+BV/ TV (%)
50
40
30
20
10
0
Empty
BCP
BCP + Pedicle
BCP + SVF + Pedicle

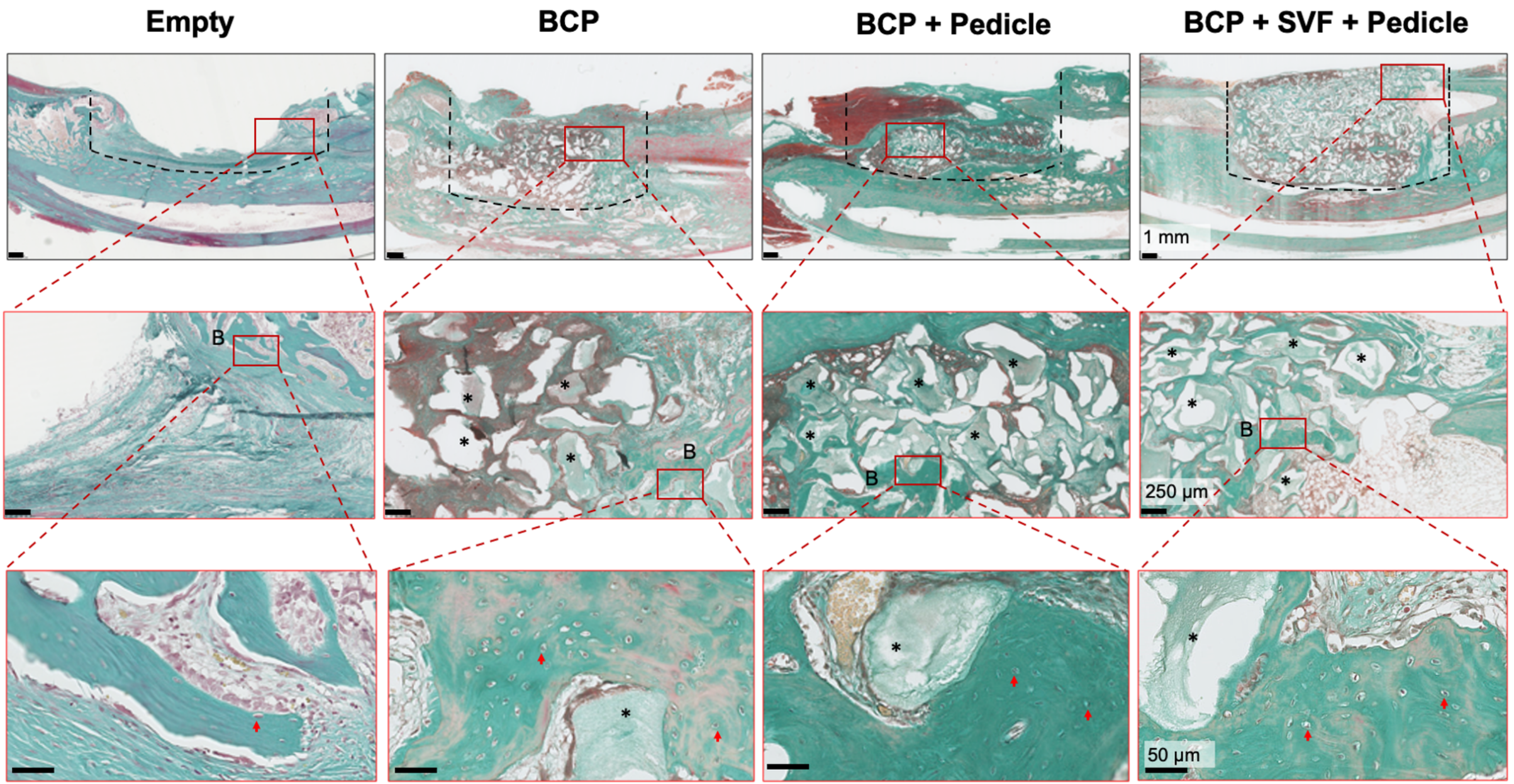
Empty
BCP
BCP + Pedicle
BCP + SVF + Pedicle
1 mm
B
B
B
250 µm
50 µm

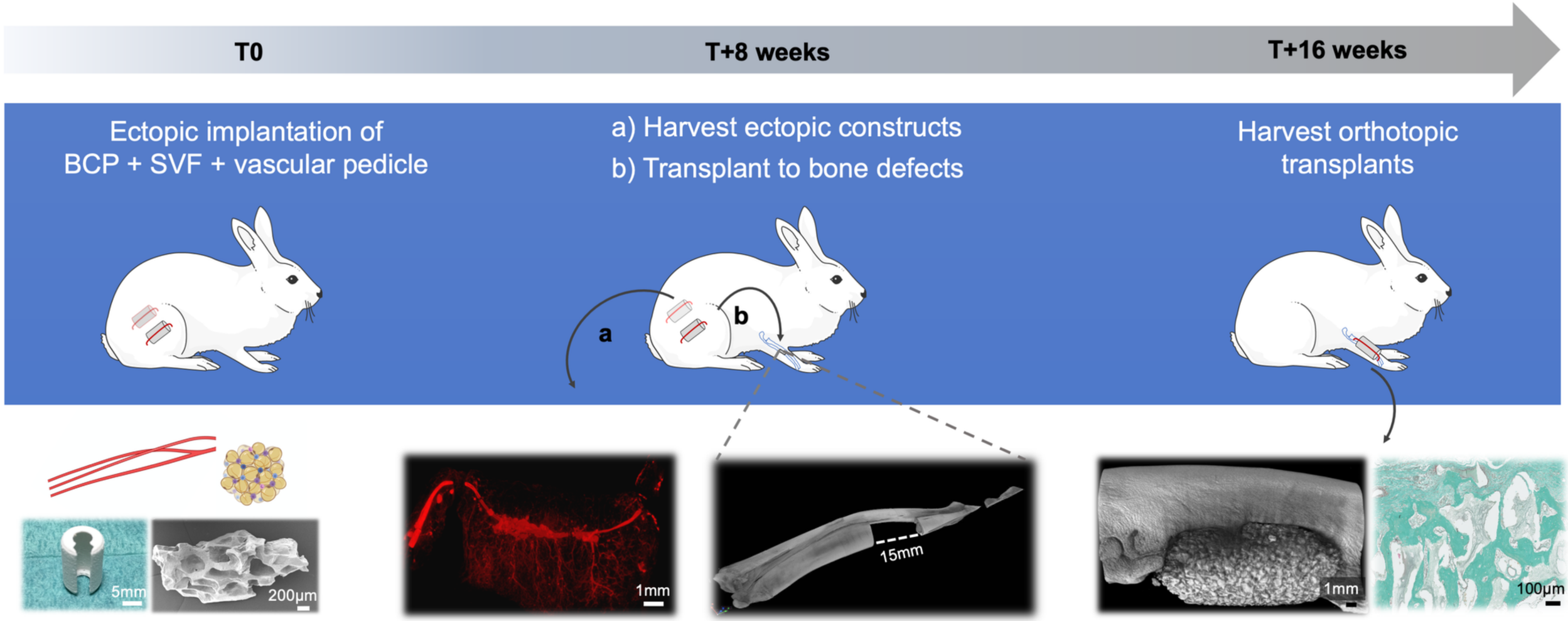
T0
T+8 weeks
T+16 weeks
Ectopic implantation of
BCP + SVF + vascular pedicle
a) Harvest ectopic constructs
b) Transplant to bone defects
Harvest orthotopic
transplants
a
b
5mm
200μm
1mm
15mm
1mm
100μm